Full-condition monitoring and intelligent yield prediction and decision-making technology for wheat combine harvesters

Weipeng Zhang[1], Hongze Guo[1], Bo Zhao[1*], Liming Zhou[1], Fengzhu Wang[1], Dongyang Wang[2], Yangchun Liu[1]

(1. *State Key Laboratory of Agricultural Equipment Technology, Chinese Academy of Agricultural Mechanization Sciences Group Co., Ltd., Beijing 100083, China*;
2. *College of Automotive and Transportation Engineering, Shenzhen Polytechnic University, Shenzhen 518055, China*)

Abstract: Against the backdrop of precision agriculture and the development of intelligent agricultural machinery, current domestic monitoring systems for wheat combine harvesters are plagued by limited functionality, low intelligence, significant errors in parameter monitoring, and yield estimation results prone to inaccuracies. Specifically, they lag behind mature international systems in terms of fault warning accuracy, data transmission efficiency, and yield visualization capabilities. This study seeks to realize comprehensive and precise monitoring, reliable fault early warning, and intelligent yield prediction for wheat combine harvesters across all operating conditions. To this end, it innovatively adopts CAN bus integration technology and impulse-type grain flow sensors to develop a comprehensive system for monitoring the operational status and warning faults of wheat combine harvesters, which covers the entire operational process. By integrating GPS positioning, multi-sensor parameter acquisition, and intelligent analysis modules through CAN bus integration, the system enables unified monitoring of geographic information, operational data, cleaning loss, and fault status. Additionally, it incorporates a yield measurement module based on an impulse-type grain flow sensor to generate the real-time yield distribution maps. Field experiments demonstrate that the system achieves an alarm accuracy of 97.3%, controls the fuel consumption measurement error within 5%, and limits the relative error of yield measurement accuracy to no more than 4%. Notably, the impulse-type grain flow sensor exhibits stable static detection accuracy and rapid, precise dynamic measurement performance—laying a solid foundation for the automation and intelligent advancement of combine harvester technologies.

Keywords: combine harvester, working condition monitoring, GPS, production forecast, intelligent decision-making
DOI: 10.25165/j.ijabe.20251806.8780

Citation: Zhang W P, Guo H Z, Zhao B, Zhou L M, Wang F Z, Wang D Y, et al. Full-condition monitoring and intelligent yield prediction and decision-making technology for wheat combine harvesters. Int J Agric & Biol Eng, 2025; 18(6): 202–211.

1 Introduction

Combine harvesters are a type of agricultural machinery widely used in modern agricultural production, greatly improving crop harvesting efficiency while alleviating labor intensity. However, the operation of combine harvesters involves substantial maintenance and management tasks, and significant challenges remain in their remote operation and management[1]. An overview of international research reveals that systems such as John Deere's Green Star and CLAAS's CEMOS have integrated functions including yield monitoring, satellite navigation, and feed rate control. Nevertheless, their core technologies are designed for the large-scale operational scenarios typical of European and American farms, exhibiting limited adaptability to China's complex field conditions—such as fragmented land parcels and hilly terrain. Domestic research has advanced in specific technologies such as the piezoelectric grain flow sensor developed by China Agricultural University and the threshing drum torque monitoring device designed by Jiangsu University[2,3]. However, most domestic monitoring systems are limited to monitoring only single parameters, such as engine speed or grain flow. They lack the capability to realize coordinated collection of multiple parameters like header height, threshing drum torque, and feed rate and thus cannot comprehensively reflect the overall operational status of the harvester.

With the development of agricultural IoT technology and agricultural informatization[4-6], mechanized agricultural production can utilize remote monitoring and data analytics to collect real-time field information and harvester operational status. Connected terminals transmit data to platforms for large-scale storage and processing[7], where platforms aggregate various types of data to support tasks such as harvester operation scheduling and yield forecasting[8-10]. This approach establishes a continuous, stable, and reliable multi-information acquisition method for combine harvesters[11], effectively managing operational condition information and thereby improving the utilization efficiency of agricultural production resources[12]. Furthermore, online monitoring technology facilitates real-time monitoring of harvester operational parameters and enables rapid acquisition of operational data in the event of equipment malfunctions[13].

Received date: 2024-01-06 **Accepted date:** 2025-11-30
Biographies: **Weipeng Zhang**, Engineer, research interest: agricultural machinery collaboration, Email: zhangwellp@163.com; **Hongze Guo**, MS candidate, research interest: automatic agricultural machinery, Email: johnguohz@163.com; **Liming Zhou**, Researcher, research interest: intelligent control of agricultural machinery, Email: haibo1129@163.com; **Fengzhu Wang**, Senior Engineer, research interest: intelligent measurement and control of agricultural machinery, Email: wangfengzhu1@126.com; **Dongyang Wang**, Lecturer, research interest: agricultural equipment engineering, Email: zpt_wdy@szpu.edu.cn; **Yangchun Liu**, Researcher, research interest: agricultural equipment measurement and control, Email: lyc327@163.com.
***Corresponding author: Bo Zhao**, Researcher, research interest: agricultural robot. Chinese Academy of Agricultural Mechanization Sciences Group Co., Ltd., Beijing 100083, China. Tel:+86-15210666162, Email: zhaoboshi@126.com.

This paper presents the design of a comprehensive operational condition monitoring and intelligent yield prediction decision-making system for wheat combine harvesters, based on Controller Area Network (CAN) bus technology[14,15]. Its innovative breakthroughs are reflected in three key aspects: First, we develop a collaborative architecture integrating multi-source sensing and the CAN bus to enable the synchronous collection of geographic data, operating condition data, and yield data, addressing the limitation of single-parameter monitoring[16-19]. Second, we establish a correlation model between yield and operating conditions, thereby realizing the bidirectional prognosis of abnormal operating conditions and yield shadow. Third, we introduce the innovation of a non-disconnecting torque sensor installation scheme[20], while integrating yield visualization and fault early warning functions[21-25]. Additionally, this study employs an impulse-based grain flow detection method and designs an impulse-type grain flow sensor system characterized by low measurement errors and high fault alarm accuracy[26,27].

Through the development and application of this system, this study aims to overcome the current technical bottlenecks in combine harvester monitoring systems—namely, fragmented parameter monitoring[28], disconnected data transmission, and non-integrated functional modules—thereby enhancing the intelligence and precision of wheat harvesting processes. This work thus provides technical support for the independent research and development of precision agricultural equipment in China.

2 Overall design of intelligent yield measurement system

2.1 System integration design

The core logic encompasses three sequential steps: first, collecting data via multi-source data acquisition; second, transmitting the collected data through a bus; and third, outputting it in a visualized manner following intelligent processing. As illustrated in Figure 1, the GPS receiver obtains geographic coordinates (latitude and longitude), while the vehicle speed sensor is used to measure the travel speed of the harvester. Using the cutting width as input, the system calculates the cumulative harvested area. Communication with the personal computer is realized through a serial port, which supports the storage of raw data and retrieval of the harvester's operational parameters. The developed impulse-type grain flow sensor continuously monitors and processes yield-related signals. The speed sensors included in the system are the elevator speed sensor, unloading chute speed sensor, and feed roller speed sensor; all these sensors communicate via the RS-485 bus without the need for protocol conversion. The photoelectric switch, which is used to detect the lifting status of the harvester's header, outputs a digital signal. Thus, a 4-channel RS-485 relay module is required to convert this digital signal into RS-485-compatible communication. Ultimately, all sensors are connected to the RS-485 Bus. The data collected through the RS-485 Bus is transmitted to a serial server, which then communicates with the monitoring system of the host computer's configuration software detection system, which in turn generates yield curves and distribution maps, thereby completing the data acquisition process and information visualization for all connected sensors.

2.2 Hardware structure design of the system

As illustrated in Figure 2, the core hardware components of the grain measurement module in the intelligent yield monitoring system comprise a sensor unit, data acquisition units, an RS485 Bus, and a grain yield display terminal. This hardware configuration constitutes an enhancement and refinement of the hardware setup employed in the first-generation yield monitoring system. Specifically, the elevator speed sensor, unloading speed sensor, and grain bin level sensor are respectively mounted on the combine harvester's elevator, unloading chute, and grain bin. These sensors directly capture physical state signals, such as the auger speed (of

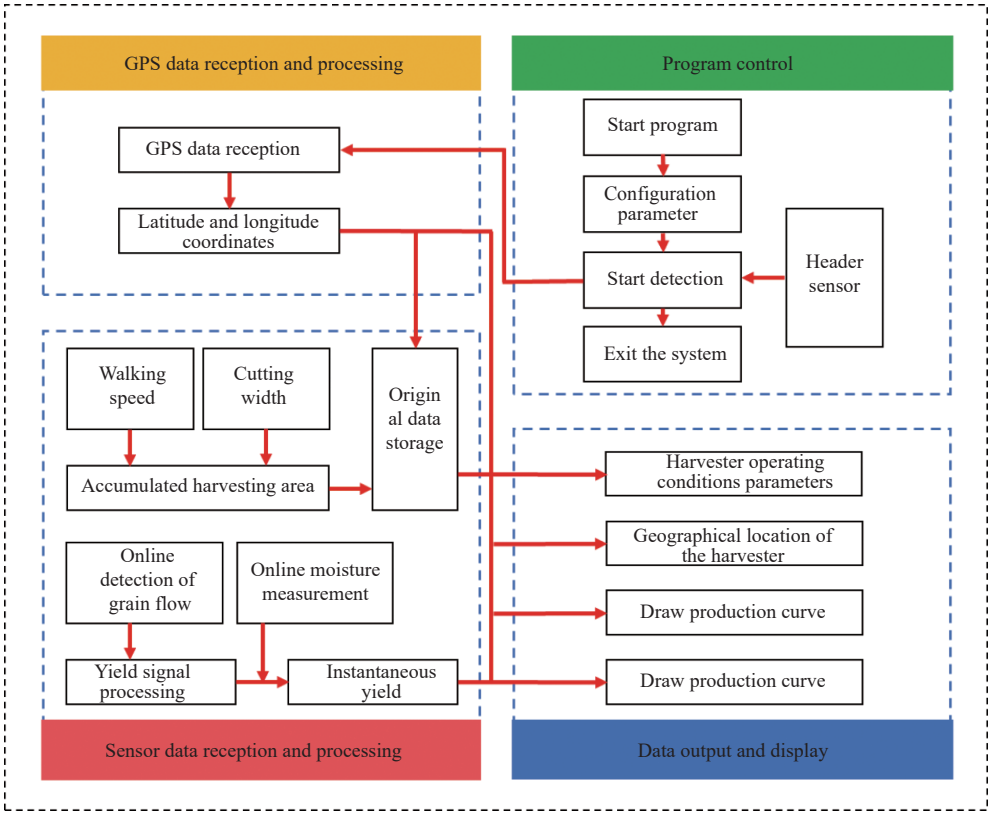

Figure 1 Overall structure frame diagram of the system

the elevator), unloading chute speed, and grain bin level height. The GPS receiver is directly connected to the data acquisition unit, providing positioning data including latitude/longitude coordinates and harvester travel speed—this data is utilized for geotagging yield measurement results and calculating the harvested area.

Signals from the sensor units are first subjected to filtering and voltage stabilization processes, followed by transmission to the data acquisition unit via the RS-485 bus. Real-time yield data is displayed on the terminal installed in the operator cab of the harvester. When faults occur, such as when the threshing cylinder speed drops below a preset threshold, an audible and visual alarm is activated. The GPRS module interacts with the data acquisition unit to receive processed operational data and yield-related data. Concurrently, it establishes a connection to a remote server-based monitoring platform through mobile communication networks. This platform receives all data uploaded by the GPRS module and supports multiple key functions: archiving historical operational records and fault logs; conducting yield comparison analyses between different fields; and adjusting operating routes according to spatial yield distribution patterns.

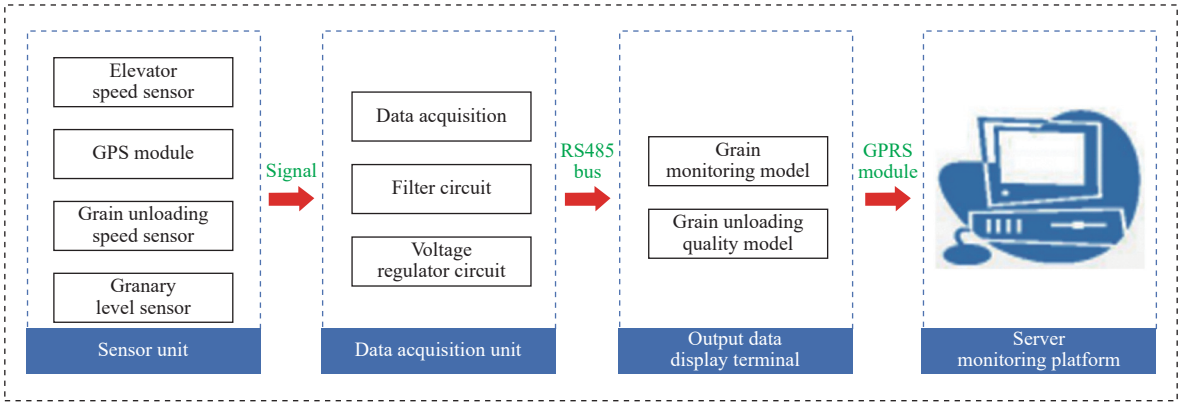

Figure 2 Composition diagram of system hardware

The core reasons for selecting the CAN bus are as follows: First, agricultural machinery operates in environments with strong electromagnetic interference, such as that generated by engines and motors. The CAN bus employs differential signal transmission, thereby providing superior anti-interference capability. Second, it supports multi-node access, enabling the simultaneous transmission of diverse sensor data to meet the requirements of "comprehensive monitoring". Third, its high transmission rate (1 Mbps) ensures that fault information is transmitted to the display and control terminal within 100 ms.

The CAN module's hardware configuration primarily consists of a master node which incorporates an STM32F103 microcontroller, which is installed in the electrical control box of the cab and integrates two CAN interfaces: CAN1 for sensor data acquisition and CAN2 for communication with the display/control terminal. Slave nodes are integrated into individual sensors and perform signal conditioning tasks, such as the amplification and filtering of torque signals. The communication protocol defines 32 types of data frames. Among them, the fault warning frame has the highest priority, with a transmission cycle of 100 ms, while general parameter frames like fuel consumption and rotational speed operate with a 500 ms transmission cycle.

2.3 System software design and hardware-software integration

The software-based data processing module utilizes algorithms to mitigate interference and errors inherent in raw data transmitted by hardware: Wavelet filtering mitigates the adverse effects of machine vibration on grain flow signals; moisture compensation models calibrate yield values based on moisture content data collected by hardware; spatiotemporal matching algorithms correlate GPS coordinates with yield data, generating location-yield association data that provides precise support for subsequent decision-making processes.

The software accommodates different hardware models via parameter configuration. When replacing a speed sensor model, the software can adjust the conversion coefficient between pulse signals and rotational speed through the human-machine interface, eliminating the need for hardware replacement. Hardware facilitates the expansion of software functions via standardized interfaces: the integration of new sensors merely requires their connection to the RS-485 bus, while the software only needs the addition of corresponding parsing modules—this ensures compatibility and flexibility during functional upgrades.

Specifically, the hardware serves as the raw data input source for the software. The software then processes the raw data via algorithmic computations to generate decision-making commands. Subsequently, these commands actuate the hardware to perform execution actions or parameter adjustments, thereby forming a comprehensive closed-loop chain spanning from monitoring through decision-making to control. Such a closed-loop architecture ensures the stable and reliable operation of the system under practical operating conditions.

The unique contributions of this research in hardware-software co-design are as follows: First, it achieves compatibility and integration across multiple sensor types, with a data acquisition coverage rate of 95%. Second, it proposes a multi-parameter threshold fusion algorithm, which reduces the fault identification time to 0.8 s. Third, it enables the cloud platform to support real-time terabyte-scale data storage and offline analysis, with a processing latency of ≤1 s.

2.4 Generation of yield distribution map

In order to achieve the objective of enhancing grain yield, it is essential to conduct in-depth analysis of spatial and temporal variations in farmland yield, identify key factors contributing to yield fluctuations, and implement site-specific zoned management of farmland and achieve the goal of increasing grain production. Notably, measurement inaccuracies during data acquisition compromise the accuracy of yield maps; therefore, the raw data employed for yield map generation necessitates preprocessing, as illustrated in Figure 3. This preprocessing encompasses four core

steps: optimization of wavelet filtering algorithms, mitigation of machine-induced vibration interference, development of moisture compensation models, and improvement of measurement accuracy.

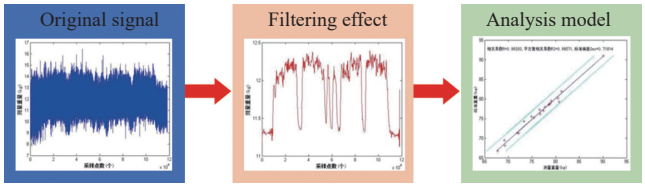

Figure 3 Signal processing flow

As shown in Figure 4, when the working condition operation monitoring and yield measurement module is working, the yield map can be generated according to the real-time yield and the corresponding GPS coordinates. The GPS positioning records all the trajectory points passed by the harvester when harvesting wheat during the operation, which can be roughly divided into three plots, in basically the north-south direction.

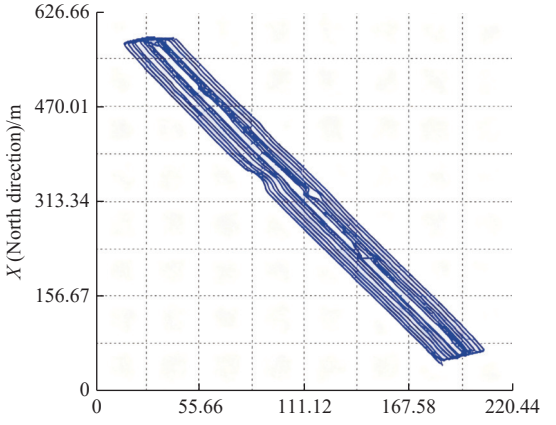

a. GPS trajectory map

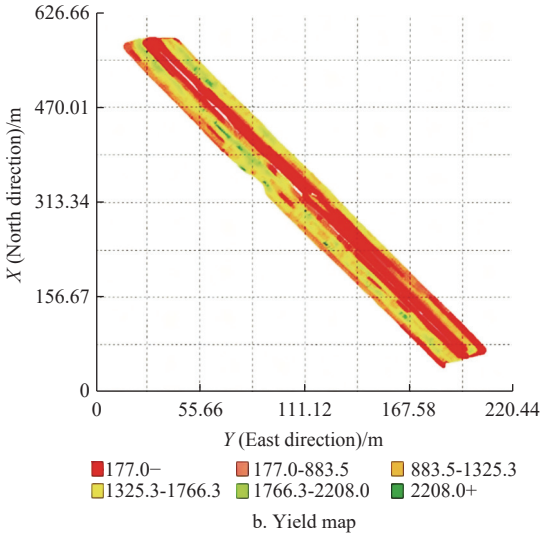

b. Yield map

Figure 4 Visual operation diagram of yield measurement

Upon acquisition of analog sensor signals, digital filtering and linear interpolation are initially applied to eliminate outliers from the flow signal. Subsequently, real-time GPS data is parsed to extract key fields—including “longitude”, “latitude”, and “time”—from its data structure, which are then converted into actual coordinate values. Finally, according to the preset time interval, field yield data is periodically transmitted to the remote server, with the format of GPRS transmission frames defined accordingly.

3 Key parameter monitoring

3.1 Monitoring device for engine output power

The output power of the combine harvester engine can be calculated by monitoring the torque and speed of the engine output shaft. Two sets of couplings are used in the torque detection, as shown in Figure 5. The sensor with a torque signal coupler is mounted between the power source and the load. In terms of installation concentricity, the specification shall be ≤ 0.1 mm.

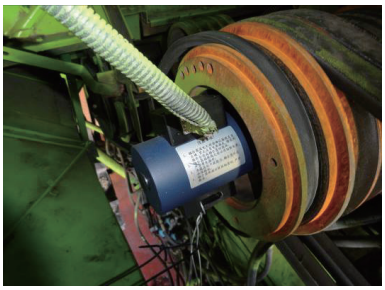

Figure 5 Installation diagram of torque sensor

If the harvester fails, it is mainly caused by the excessive load in the threshing cylinder and the auger. When the power of the diesel engine is strong and the load in the drum or auger is not very large, the speed of the diesel engine decreases slowly. When the load exceeds the critical value, the degree of decline gradually becomes faster, and the drum will be blocked due to excessive load. According to this principle, the rotational speed data of the drum auger of the harvester is monitored, and the monitoring results are shown in Figure 6.

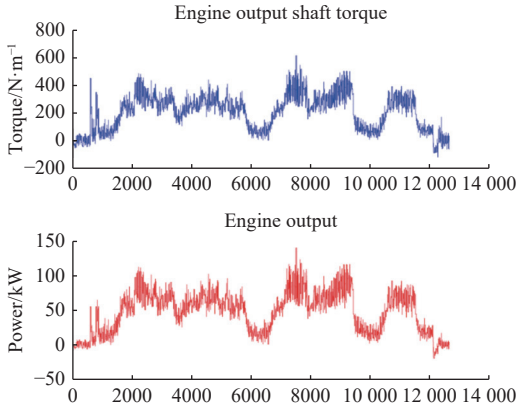

Figure 6 Real-time monitoring curve of engine output shaft

3.2 Torque monitoring device

In order to accurately obtain the working condition and workload of the harvester and give early warning of abnormal situations, it is necessary to use the torque sensor to obtain the real-time torque information of each rotating shaft. The threshing working parts of combine harvester are mainly the double longitudinal axial flow threshing drum. In order to monitor the threshing power of the combine harvester, a torque monitoring device for the power drive shaft of the longitudinal axial flow threshing drum was designed. In the traditional torque sensor, the sensor needs to be connected in series between the power source and the load in the form of broken shaft, which will bring great inconvenience to the installation of the sensor. The torque sensing detection device in this study can be directly installed on the outside of the transmission wheel without disconnecting the transmission

shaft. The principle is shown in Figure 7. The core mechanism relies on the combination of non-contact signal acquisition and strain sensing-frequency conversion, enabling precise monitoring of torque data.

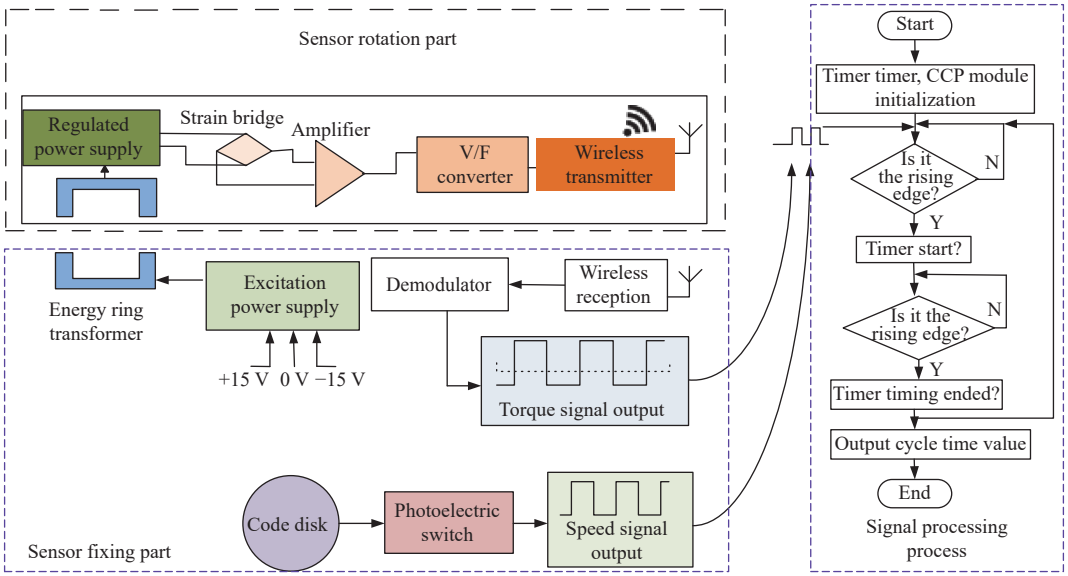

Figure 7 Principle of torque sensor

On the elastic shaft segment of the rotor assembly, four strain gauges are symmetrically bonded—two at 45° and two at 135° relative to the axial and circumferential directions—thereby forming a full-bridge measurement circuit. When the drive shaft is subjected to torque, the elastic shaft undergoes corresponding torsional deformation: the strain gauges oriented at 45° are subjected to tensile stress with an increase in resistance, while those oriented at 135° experience compressive stress with a decrease in resistance. The full-bridge circuit outputs a differential voltage signal that is proportional to the applied torque. This signal is first amplified via an amplifier, then converted into a voltage-to-frequency (V-F) output by a signal converter, and finally received and demodulated by a wireless receiver to acquire real-time torque signals.

The installation diagram of the transmission shaft of the header is shown in Figure 8. The disc torque sensor is installed at the header shaft by breaking the shaft, and the two ends of the rotor are connected with the left and right half shafts through the flange coupling respectively. Figure 9 is the installation diagram of the torque sensor at the threshing drum shaft. The threshing drum shaft of the harvester is a complete pipe shaft welding part, which is not suitable for the broken shaft installation method. The short shafts are lengthened to realize the power output. This component is fixed to the sensor rotor through a keyed connection, ensuring synchronous rotation of the rotor with the drive shaft and preventing potential torque transmission errors resulting from relative slippage. The drum output power and torque real-time monitoring curve are shown in Figure 10.

Figure 8 Torque monitoring of header barrel

Figure 9 Threshing drum on-line monitoring device

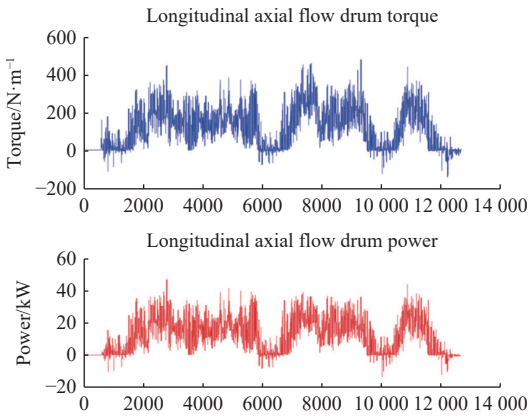

Figure 10 Real-time monitoring curve of longitudinal axial flow drum

3.3 Height of header

The stubble height refers to the height from the top of the stubble left in the plot to the ground after wheat harvest. The header height sensor is a displacement sensor of type KTM75, linear accuracy: 0.05%, repetitive linear accuracy: 0.01 mm, measurement length: 0-75 mm, output type: 0-given input working voltage, working temperature: −30°C to 125°C. In this paper, the cable displacement sensor was used to measure the elongation of the hydraulic cylinder of the header, and the linear relationship model was established between the stubble height and the elongation of the

hydraulic cylinder of the header based on the least square fitting algorithm.

$$h = a_1 + a_2 r \tag{1}$$

where, h is cut stubble height, mm; r is cutter hydraulic cylinder elongation, mm; a_1, a_2 are constants determined by calibration test.

The position sensor of the cutting table also uses the proximity switch to judge the lifting state of the cutting table. When the header is lifted, the yield data acquisition is stopped to avoid the abnormal working state of the harvester during the turning process in the ground and affect the measurement accuracy.

3.4 Positioning device

The main function of the positioning receiver is to position the harvester in real time and record the geographical coordinates corresponding to the current yield value according to the data acquisition frequency of the yield measurement system, which is the positioning information in the yield data.

Beijing Unicore UM220-Ⅲ dual -system navigation/timing module was selected in the module, mainly for locating the vehicle position of combine harvester and calculating the vehicle speed. Dual-system, multi-frequency, and high-performance SOC chip was adopted in UM220-Ⅲ, which supports BD2B1 and GPS L12 frequency points at the same time, and provides two UART output interfaces, with a positioning accuracy of 25mCEP, high integration, and low power consumption, which is very suitable for occasions with high positioning performance, product reliability, and quality requirements. The multi-objective decision-making and control logic of the system is illustrated in Figure 11.

3.5 Principles for sensor system selection and installation

The output types of each sensor in the system mainly include 12 V torque frequency signal, 12 V speed pulse signal, NPN voltage output pulse signal, and 4-20 mA current signal, as listed in Table 1. Based on PIC26K80 controller, 7-channel frequency acquisition module and 8-channel analog acquisition module were designed based on CAN bus output in this paper, and a vehicle-mounted CAN channel network was constructed for hardware signal acquisition of various sensors, which meets the overall data acquisition needs of the system. The overall installation layout of the harvester's internal sensor system is presented in Figure 12. For installation specifics: the Hall-effect speed sensor must be fastened with an L-shaped bracket to avoid collisions caused by excessive proximity or signal loss due to excessive distance. The fuel consumption sensor is installed with a rubber shock-absorbing bracket to mitigate the interference of engine vibrations on measurement accuracy.

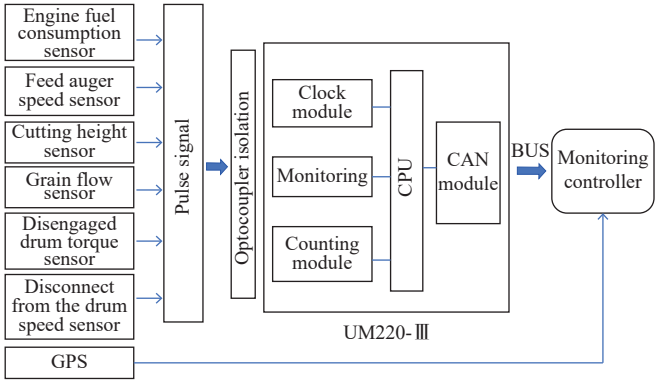

Figure 11 Multi-objective decision-making and control logic diagram

Table 1 Core sensor selection and installation

Sensor	Model	Core parameters	Detection range	Installation location
Height of cutting stubble	KTC400 guyed displacement sensor	Linearity≤0.2%; Lifespan≥ 500 000 cycles	0-1500 mm	Lifting support
Working shaft speed	Hall speed sensor	Response frequency: 0-10 kHz; Triggering magnetic field≥20 mT	0-3000 r/min	Roller end cap
Engine fuel consumption	LWGY-15 Turbine Flowmeter	Output signal: Pulse (0.1-5 kHz); Material: 304 Stainless Steel	0-50 L/h	Fuel inlet pipe
Positioning and forward speed	UM220-III Dual-System GPS	Receiving frequency: GPS L1/CNS B1; Refresh rate: 1 Hz	Positioning accuracy: 1 m; Speed accuracy: 0.1 m/s	Roof of the cab
Grain flow	YL-100 Impulse Sensor	Output signal: 4-20 mA current; Protection rating: IP67	0-10 kg/s	Elevator outlet
Working shaft torque	HX -900 Rotary torque sensor	Output signal: 0-5V voltage; Operating temperature: −40°C to 85°C	0-1500 N·m	Extended short shaft

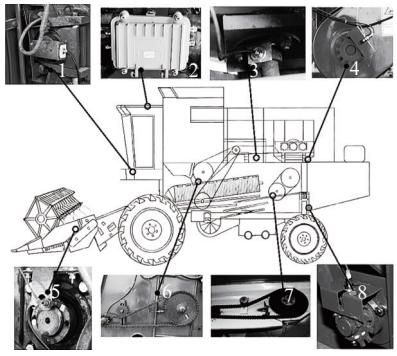

1. Grain flow sensor 2. CAN Bus 3. Threshing drum sensor 4. Elevator auger speed sensor 5. Cutter height sensor 6. Cutting drum speed sensor 7. Grain discharge auger sensor 8. Engine fuel consumption sensor

Figure 12 Internal layout diagram of the sensing system

4 Intelligent decision technology

4.1 Establishment of grain trajectory model after being thrown off the scraper

Through the analysis of the movement process of the grain flow in the whole elevator conveying system, the trajectory of the grain after being thrown off the scraper is parabolic. Because the terminal velocity and angle are different when it is thrown off the scraper and the initial speed of the final grain when it is thrown off the scraper is determined by the linear speed of the elevator and the speed when the grain slides to the end of the scraper, it is necessary to analyze the speed when the grain is thrown off the scraper. Assuming that the throwing points of the grains thrown off the scraper at different positions are their respective coordinate dots, the formula for calculating the initial speed of the grains thrown off is:

$$v_H = \sqrt{v_Q^2 + v_0^2} \tag{2}$$

where, V_H in the hypothetical formula is the actual speed of the grain when it is thrown off the scraper; V_Q is linear velocity at the end of scraper, m/s; V_0 is the speed when the grain slides to the end of the scraper, m/s.

Assuming that the grain is only influenced by gravity, ignoring factors such as air resistance and collision between grains, the motion equation of the grain is:

$$x = v_H \cos\beta \cdot t \tag{3}$$

$$y = v_H \sin\beta \cdot t - \frac{1}{2} g t^2 \tag{4}$$

where, y is the vertical distance of parabolic motion, m; x is horizontal distance of parabolic motion, m; β is included angle between actual grain speed and horizontal direction, the unit is degrees; t is time for the grain to make parabolic motion, m; g is acceleration of gravity, m/s^2; V_a is initial speed when the grain is thrown off the scraper, m/s.

Then the trajectory equation of the grain after being thrown off the scraper is:

$$y = \tan\beta \cdot x - \frac{g}{2} \cdot \frac{x^2}{v_a^2 \cos^2\beta} \tag{5}$$

Synthesizing the above types, the trajectory of grains at different positions after being thrown off the scraper can be calculated, which can provide theoretical basis for the design of structural parameters of impact plate of impulse grain yield sensor.

4.2 Dynamic measurement of output

Real-time monitoring of grain loss during the field operations of combine harvesters is critical for improving harvesting efficiency and quality. The grain sensing system acts as the core component for yield monitoring and operational condition identification, which primarily consists of a PVDF array-based sensor, signal conditioning modules, communication interfaces, and display devices.

The PVDF piezoelectric film sensors utilized in this system exhibit a five-layer structure: two protective PET layers that sandwich a central PVDF pressure film layer, with a rubber layer and an aluminum alloy substrate layer underneath, which collectively provide vibration damping and structural support as shown in Figure 13. When the grain flow impinges on the sensor surface, the generated impulse is transduced into an electrical signal. The momentum principle underpinning this process can be expressed as: The impulse acting on the sensor equals the product of the grain mass and the impact velocity of the grain stream.

The mechanical principle of the dual-plate differential impulse grain flow sensor is as follows: The grain is conveyed to the top of the silo via a grain elevator. Grain traveling at a specific velocity is projected onto the impact plate of the flow sensor. As grains periodically strike the impact plate, the resistance of strain gauges affixed to its rear surface varies with the deformation of the plate. An amplifier transmits this force signal to an A/D converter, which converts it into digital data stored in the computer memory as shown in Figure 14. Experimental tests demonstrate the sensor's high measurement accuracy and response speed, while simultaneously capturing the spatial distribution information of the grain.

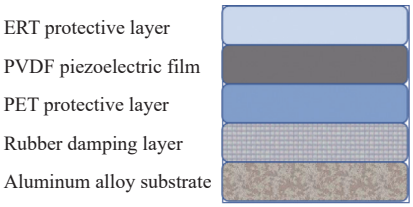

Figure 13 PVDF sensor unit structural diagram

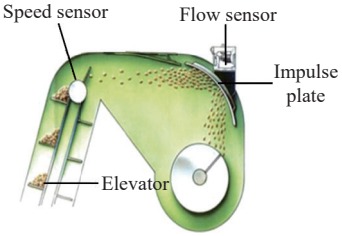

Figure 14 Schematic diagram of monitoring process of impulse yield measurement module

4.3 Decision model of feeding amount measurement

The feeding amount is the mass of materials fed into harvesting machinery in unit time, and its acquisition will be affected by the physical characteristics of materials such as material humidity and grain-grass ratio. As shown in Figure 15, the rotational speed or torque of the threshing drum is used to represent the feeding amount. When the model of the combine harvester is determined and the physical characteristics of the material are constant, there is a one-to-one correspondence between the oil pressure and the feeding amount, and the theoretical equation can well reflect the feeding amount. If the physical characteristics of materials change, even if the feed rate remains unchanged, the changes in the friction coefficient, compression coefficient, grain-grass ratio, and natural laying density of non-grain materials will affect the oil pressure, thus affecting the judgment of feeding amount.

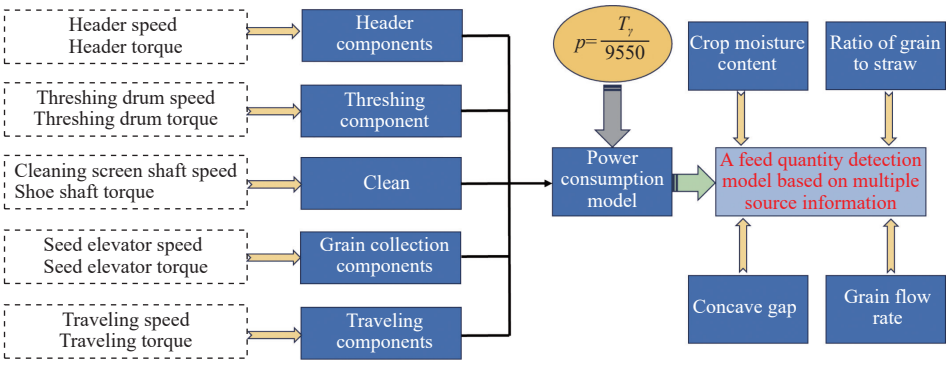

Figure 15 Feeding amount detection model based on multi-source information fusion

5 Analysis of field trial results

In August 2022, a two-day wheat harvesting field trial was conducted at the experimental site of Shengli Farmers' Cooperative in Dezhou, Shandong Province. During the trials, under clear and rain-free weather conditions, the comprehensive performance of the

online monitoring and automatic fault warning system for wheat harvesters was tested.

The experimental equipment was a Lovol Gushen self-propelled wheat combine harvester equipped with this monitoring system, featuring an engine power of 160 kW, a rated speed of 2200 r/min, and a header width of 4.5 m. Field levelness was measured using a laser level, with a tolerance of ±5 cm. Prior to the experiment, uniform baseline parameters were established as reference standards for evaluating the monitoring system's performance, in accordance with GB/T 21961-2020 (*Test Methods for Combine Harvesters*). The specific experimental plan and assessment criteria are listed in Table 2.

Table 2 Experimental schedule

Experimental phase	Interim objectives	Content	Methods	Performance indicators
Preliminary experimental	System debugging to eliminate hardware faults	CAN bus data transmission testing; pre-operation of filtering and compensation algorithms	Transmit test data packets to measure packet loss rate; import simulated data to validate algorithm output accuracy.	CAN bus packet loss rate ≤ 0.1%; algorithm simulation output error ≤ 1%.
Performance testing	Testing the core performance of the monitoring system	Monitoring accuracy testing and continuous operational stability testing	Simultaneously collect sensor data and weighing instrument data to calculate relative error; continuously run to statistically determine the number of data anomalies.	Monitoring error ≤3.5%, torque accuracy ≤0.8%; number of anomalies within 8 h ≤2
Field validation	Verify the effectiveness in actual operations	Simulated fault warning response; production chart generation and accuracy verification	Manually adjust parameters and record alert conditions; generate yield maps by statistically analyzing zone-specific net yield loss rates and loss rates, and compare these with field-sampled yields.	Fault warning accuracy ≥95%, response time ≤200 milliseconds; production chart error ≤4%.
Data processing	Data collation and analysis	Experimental data screening to eliminate outliers; identification of error sources and assessment of compensation effectiveness	Apply the 3σ rule to exclude outliers; compare the change in error before and after compensation.	Data validity rate ≥ 95%; compensated error reduction ≥ 40%.

As shown in Figure 16, the grain conveying system of the wheat combine harvester equipped with this precision harvesting system operates smoothly without any blockages. The test results show that the on-line monitoring system of the working condition of the wheat combine harvester runs normally, and the working performance of the detection devices such as the speed sensor, power detection sensor, and torque sensor is good, which meets the functional requirements and accuracy requirements of the field operation condition monitoring.

Figure 16 Harvesting test site

However, when the measurement system traverses areas with undulating slopes, yield measurement results exhibit slight discrepancies. Subsequent analysis indicates that this discrepancy may originate from grain segregation within the elevator, which in turn causes increased load on one side of the flow sensor. It is therefore recommended that slope sensors be installed during field operations in hilly regions, where tilt compensation can be employed to enhance the accuracy of yield detection.

5.1 Operation fault monitoring

When the fault occurs, the speed mutation trend of the drum and the auger of the harvester is the same. According to the blockage situation on site, it is found that the drum is full of crops, while the crop volume in the auger is normal and there is still a large space. It can be determined that the drum blocking is caused by the large load of the drum, and the drum and the auger share a driving shaft, so the drum blocking will react to the driving shaft, and then the speed of the auger will also decrease. Therefore, the monitored curve is consistent with the actual situation, which verifies the feasibility of monitoring the harvester by the system.

As shown in Table 3, the field test shows that the system can perform sound and light alarm prompts under fault conditions. Through the vehicle display terminal, the operator can grasp the working conditions of the whole machine, as well as the working load and fault state of each key mechanism in real time, and make timely adjustment and treatment, which reduces the incidence of field harvest faults and improves the operation efficiency.

Table 3 Agricultural machinery fault alarm test

Rated speed of threshing cylinder r·min^{-1}	Actual speed of threshing cylinder r·min^{-1}	Voice prompt information
600	597	none
600	501	none
600	540	none
600	378	alarm
600	330	alarm

5.2 Visual display of yield measurement

After harvesting a field, in order to clearly and intuitively show the real-time yield distribution of the field, the real-time yield distribution map is drawn when the harvesting machine performs the harvesting task, so that the yield between the various parts of the field can be intuitively and strikingly understood. As shown in Figure 17, in order to obtain multiple sets of field test data under different operating parameters, the plot is divided into multiple test groups according to the length of 35 m and the width of 4.5 m. Each test group was set as a pre-acceleration zone (20 m), a harvest determination zone (10 m), and a stop operation zone (5 m) according to the direction of the wheat combine harvester. Among them, the wheat operations in the pre-acceleration area and the stop operation area have been pre-harvested.

The accuracy of preliminary yield maps is a fundamental prerequisite to ensure stable harvesting quality across entire fields. Subsequently, the experimental fields will be divided into distinct grid units based on yield variations, precisely delineating yield gradient zones. Each unit will be assigned specific harvesting parameters according to the preliminary yield data. High-yield gradient units will employ low-speed, high-rotation harvesting modes to effectively reduce grain loss rates, while low-yield gradient units will adopt high-speed, low-rotation modes to ensure uniform harvesting quality.

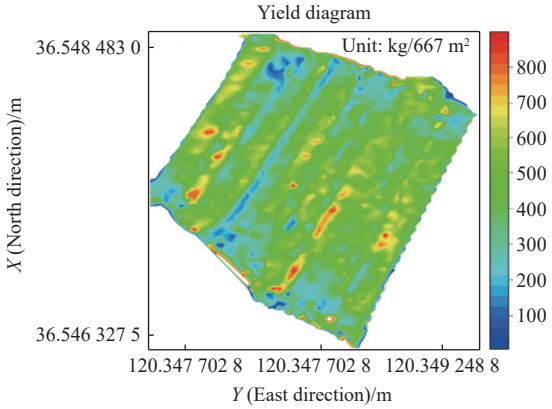

Figure 17 Visual operation diagram of field yield measurement

In the visual operational map, plot yields correlate with soil organic matter content. Weed coverage during harvesting may block GPS signals, causing coordinate deviations. The adjacent point interpolation method is used to correct such deviations, limiting data errors to within 2%.

5.3 Validation test of grain yield measurement performance

In accordance with the general specifications of GB/T 5262-2008 (*Test Conditions and Methods for Agricultural Machinery*), the five-point sampling method shall be adopted, where each sampling point covers an area of 1 m^2. The field harvest yield test of the system was carried out five times, with each harvest mass between 500-1500 kg. The yield monitoring value was recorded after each harvest, and the grain was unloaded to the grain collection box when the grain was returned to the field to be weighed to obtain the actual harvest value. During the experiment, the yield of wheat field was selected for harvesting and the quality was weighed. The experimental data of the combine harvester in each paddy field were marked and distinguished for data analysis. Table 4 is the data of system field yield test.

Table 4 Field yield measurement results of the system

Serial number	Longitude/(°)	Latitude/(°)	Increase the speed of the auger/r·min^{-1}	Grain flow of monitoring cereals/kg·s^{-1}	Average grain flow	Total mass of monitoring grain/kg	Actual total mass of weighing grain/kg	Relative error/%
1	116.725 244	37.439 754	530	0.502 58				
2	116.729 107	37.431 794	540	0.542 24				
3	116.728 545	37.435 788	530	0.501 85	0.502 912	411.52	424.64	3.089
4	116.722 148	37.436 847	530	0.475 21				
5	116.725 89	37.433 156	540	0.492 68				

An analysis of grain flow monitoring errors revealed that the measurement accuracy is influenced by variations in wheat moisture content during the testing process. When the moisture content is high, the grain density increases, which in turn amplifies the detection signal output by the impulse-type sensor. This phenomenon leads to elevated grain flow readings and a subsequent increase in measurement errors. To mitigate this issue, a moisture compensation algorithm was then integrated into the monitoring system. This algorithm utilizes real-time data from the moisture content sensor to correct grain flow measurements, thereby effectively reducing interference from moisture-related environmental factors.

The rotational speed of the lifting auger of the combine harvester is basically maintained at 530 r/min, and the operation is stable. The wheat flow values under different positioning coordinates are different, which well reflects the differences in wheat yield in different regions of the paddy field. The experimental results show that the designed grain yield monitoring system has good overall performance, strong field adaptability, and the relative error of online yield measurement is 3.089%. The grain flow positioning is real-time and accurate, and the grain yield prescription map drawn by this method has certain credibility and practicability.

6 Conclusions and future work

This study addresses key challenges in wheat combine harvesters, including inadequate monitoring accuracy across full operating conditions, high false alarm and missed detection rates in fault early warning, and a disconnect between yield prediction and operational decision-making. Through the rational optimization of hardware integration, innovation in algorithms, and effective collaboration with cloud platforms, we have developed an integrated system encompassing data perception, data transmission, data post-processing, and ultimate decision-making.

Compared with existing technologies, this innovation achieves breakthroughs in non-disconnect shaft-based multi-source sensor integration. By welding extended short shafts to accommodate rotary torque sensors, non-disconnect shaft installation is realized without damaging the original shaft system. Integrated impulse-type flow sensors are uniformly connected via CAN/RS-485 buses, yielding installation compatibility with over 90% of domestic combine harvester models. By overcoming the challenges of false alarms and false negatives inherent in traditional fixed-threshold methods, we have developed a multi-parameter synergistic dynamic early warning algorithm, which consists of three core modules: multi-dimensional feature extraction, adaptive dynamic thresholding, and multi-trend prediction. Additionally, this innovation incorporates IoT cloud-based decision-making, linking operational status, grain yield, and geographic location via detailed yield distribution maps. This provides data support for future precision fertilization, harvesting path planning, and field zoning management.

Future research may extend this system to harvesting diverse crops such as coarse-stemmed corn and rice under humid conditions, achieved by adopting shock-resistant corn kernel flow sensors, waterproof rice header height sensors, and calibrating algorithmic thresholds. Concurrently, developing modular kits to accommodate hardware differences between small self-propelled harvesters and large combines will reduce deployment costs. With the advancement of IoT and big data technologies, remote interconnection between multiple harvesters will be feasible in the foreseeable future. Based on real-time field yield data, harvesters can be dynamically allocated to specific operational zones for fleet-level scheduling. Leveraging long-term accumulated fault data samples, deep learning models can be trained for automated fault classification, evolving from fault early warning to predictive maintenance. This will enable full-cycle management covering pre-harvest prediction, in-harvest monitoring, and post-harvest analysis.

This research integrates CAN bus technology and multi-sensor fusion to enable comprehensive operational monitoring, fault early warning, and yield analysis for wheat combine harvesters. Field trial results indicate that this system significantly improves operational efficiency and quality, substantially reducing the probability of work interruptions and harvesting losses due to fault-induced downtime. While directly increasing economic value per mu for farmers, the system also outputs data including "field yield distribution maps" and "operational parameter logs". These data can be integrated into regional agricultural big data platforms to support macro-level decision-making regarding water, fertilizer, and pesticide application, aligning with the development direction of green agriculture.

Acknowledgements

The work was financially supported by the National Key Research and Development Program of China Subproject (Grant No. 2022YFD200150503).

[References]

[1] Zhang Y, Yin Y, Meng Z, Chen D, Qin W, Wang Q, Dai D. Development and testing of a grain combine harvester throughput monitoring system. Computers and Electronics in Agriculture, 2022; 200: 107253.

[2] Vakhrushev V V, Nemtsev A E, Ivanov N M. Evaluation of the main indicators of the reliability of the power transmission of a combine harvester John Deere 9660. IOP Conference Series: Materials Science and Engineering, 2020; 941(1): 012068.

[3] Bai X, Chen Q, Song X, Hong W. Advancing agricultural machinery maintenance: Deep learning-enabled motor fault diagnosis. IEEE Access, 2025; 13: 129933–129951,

[4] Zhang W, Zhao B, Zhou L, Wang J, Niu K, Wang F, et al. Research on comprehensive operation and maintenance based on the fault diagnosis system of combine harvester. Agriculture, 2022; 12(6): 893.

[5] Qiu Z, Shi G, Zhao B, Jin X, Zhou L. Combine harvester remote monitoring system based on multi-source information fusion. Computers and Electronics in Agriculture, 2022; 194: 106771.

[6] Fei S, Hassan M A, Xiao Y, Su X, Chen Z, Cheng Q, et al. UAV-based multi-sensor data fusion and machine learning algorithm for yield prediction in wheat. Precision Agriculture, 2023; 24(1): 187–212.

[7] Zhu H, Liang S, Lin C, He Y, Xu J L. Using multi-sensor data fusion techniques and machine learning algorithms for improving UAV-based yield prediction of oilseed rape. Drones, 2024; 8(11): 642.

[8] Belay M A, Blakseth S S, Rasheed A, Rossi P S. Unsupervised anomaly detection for IoT-based multivariate time series: Existing solutions, performance analysis and future directions. Sensors, 2023; 23(5): 2844.

[9] Sinha B B, Dhanalakshmi R. Recent advancements and challenges of internet of things in smart agriculture: a survey. Future Generation Computer Systems, 2022; 126: 169–184.

[10] Almufareh M F, Humayun M, Ahmad Z, Khan A. An intelligent LoRaWAN-based IoT device for monitoring and control solutions in smart farming through anomaly detection integrated with unsupervised machine learning. IEEE Access, 2024; 12: 119072–119086.

[11] Zou X, Liu W, Huo Z, Wang S, Chen Z, Xin C, et al. Current status and prospects of research on sensor fault diagnosis of agricultural internet of things. Sensors, 2023; 23(5): 2528.

[12] Zhang X, Rane K P, Kakaravada I, Shabaz M. Research on vibration monitoring and fault diagnosis of rotating machinery based on internet of things technology. Nonlinear Engineering, 2021; 10(1): 245–254.

[13] Choe H O, Lee M H. Artificial intelligence-based fault diagnosis and prediction for smart farm information and communication technology equipment. Agriculture, 2023; 13(11): 2124.

[14] Yuan X, He Y, Wan S, Qiu M, Jiang H. Remote vibration monitoring and fault diagnosis system of synchronous motor based on internet of things technology. Mobile Information Systems, 2021; 2021(1): 3456624.

[15] Chen M, Jin C, Ni Y, Yang T, Zhang G. Online field performance evaluation system of a grain combine harvester. Computers and Electronics in Agriculture, 2022; 198: 107047.

[16] Mohammad Hosseinpour-Zarnaq, Mahmoud Omid, Ebrahim Biabani-Aghdam. Fault diagnosis of tractor auxiliary gearbox using vibration analysis and random forest classifier. Information Processing in Agriculture, 2022; 9(1): 60–67.

[17] Mejbel B G, Sarow S A, Al-Sharify M T, AI-Haddad L A, Ogaili A A F, AI-Sharify Z T. A data fusion analysis and random forest learning for enhanced control and failure diagnosis in rotating machinery. Journal of Failure Analysis and Prevention, 2024; 24(6): 2979–2989.

[18] Yılmaz D, Gökduman M E. Development of a measurement system for noise and vibration of combine harvester. Int J Agric & Biol Eng, 2020; 13(6): 104–108.

[19] Song Y, Zhang X, Wang W. Rollover dynamics modelling and analysis of self-propelled combine harvester. Biosystems Engineering, 2021; 209: 271–281.

[20] Badihi H, Zhang Y, Jiang B, Pillay P, Rakheja S. A comprehensive review on signal-based and model-based condition monitoring of wind turbines: Fault diagnosis and lifetime prognosis. Proceedings of the IEEE, 2022; 110(6): 754–806.

[21] Che Y, Zheng G, Li Y, Hui X, Li Y. Unmanned agricultural machine operation system in farmland based on improved fuzzy adaptive priority-driven control algorithm. Electronics, 2024; 13(20): 4141.

[22] Mikram M, Moujahdi C, Rhanoui M. Deep learning and machine learning approaches for data-driven risk management and decision support in precision agriculture. International Journal of Sustainable Agricultural Management and Informatics, 2025; 11(2): 226–247.

[23] Younas M, Akhtar M N, Batool S, Owais M, Sahar S, Anum W. The integration of artificial intelligence in agriculture: Emerging trends, benefits and challenges. Journal of Asian Development Studies, 2025; 14(1): 1316–1333. DOI: https://doi.org/10.62345/jads.2025.14.1.105.

[24] Bala A, Rashid R Z J A, Ismail I, Oliva D, Muhammad N, Sait S M, et al. Artificial intelligence and edge computing for machine maintenance-review. Artificial Intelligence Review, 2024; 57(5): 119.

[25] Li H, Gao F, Zuo G C. Research on the agricultural machinery path tracking method based on deep reinforcement learning. Scientific Programming, 2022; 2022(1): 6385972.

[26] Singh A K, Junior F N F, Mainsah N L, Abdoul-Rahmane B. Enabling data collection and analysis for precision agriculture in smart farms. IEEE Transactions on AgriFood Electronics, 2024; 3(1): 69–85.

[27] Wang H, Lao L, Zhang H, Tang Z, Qian P, He Q. Structural fault detection and diagnosis for combine harvesters: A critical review. Sensors, 2025; 25(13): 3851.

[28] Xu S, Wang H, Liang X, Lu H. Research progress on methods for improving the stability of non-destructive testing of agricultural product quality. Foods, 2024; 13(23): 3917.